A topological proof of chaos for two nonlinear heterogeneous triopoly game models

Marina Pireddu

Citation: Chaos **26**, 083106 (2016); doi: 10.1063/1.4960387
View online: http://dx.doi.org/10.1063/1.4960387
View Table of Contents: http://scitation.aip.org/content/aip/journal/chaos/26/8?ver=pdfcov
Published by the AIP Publishing

A topological proof of chaos for two nonlinear heterogeneous triopoly game models

Marina Pireddu[a)]
Department of Mathematics and Applications, University of Milano-Bicocca, U5 Building, Via Cozzi 55, 20125 Milano, Italy

(Received 9 February 2016; accepted 22 July 2016; published online 8 August 2016)

We rigorously prove the existence of chaotic dynamics for two nonlinear Cournot triopoly game models with heterogeneous players, for which in the existing literature the presence of complex phenomena and strange attractors has been shown via numerical simulations. In the first model that we analyze, costs are linear but the demand function is isoelastic, while, in the second model, the demand function is linear and production costs are quadratic. As concerns the decisional mechanisms adopted by the firms, in both models one firm adopts a myopic adjustment mechanism, considering the marginal profit of the last period; the second firm maximizes its own expected profit under the assumption that the competitors' production levels will not vary with respect to the previous period; the third firm acts adaptively, changing its output proportionally to the difference between its own output in the previous period and the naive expectation value. The topological method we employ in our analysis is the so-called "Stretching Along the Paths" technique, based on the Poincaré-Miranda Theorem and the properties of the cutting surfaces, which allows to prove the existence of a semi-conjugacy between the system under consideration and the Bernoulli shift, so that the former inherits from the latter several crucial chaotic features, among which a positive topological entropy. *Published by AIP Publishing.*
[http://dx.doi.org/10.1063/1.4960387]

In the economic literature, the study of dynamical aspects in game theory models is becoming more and more relevant, in particular, in regard to oligopoly contexts.[10,11,14,40] On the other hand, due to the complexity of the models considered, an analytical study of the associated dynamical features turns out often to be too difficult or simply impossible to perform. That is why many dynamical systems are studied mainly from a numerical viewpoint (see, for instance, Refs. 2, 4, 42, and 43). In the context of triopoly games, where the setting is given by an oligopoly composed by three firms, a local analysis can generally be performed in the special case of homogeneous triopoly models, in which the equations describing the dynamics are symmetric (see, for instance, Refs. 1, 3, and 34). A more difficult task is that of studying heterogeneous triopolies, like, e.g., those in Refs. 14–16, 18, 25, and 41, where the three firms considered behave according to different strategies. Following the line of research started in Ref. 29, in this paper we are going to complement the analysis performed in Refs. 14 and 41, where the presence of complex phenomena and strange attractors for two nonlinear Cournot triopoly game models with heterogeneous players has been shown via numerical simulations. The method we will employ in our analysis of the models in Refs. 14 and 41 is the "Stretching Along the Paths" technique, which, in particular, allows us to show the existence of a semi-conjugacy between the considered dynamical system and the Bernoulli shift, so that the former inherits from the latter the main features related to a complex behavior, i.e., positivity of the topological entropy, topological transitivity, and sensitive dependence on initial conditions, on suitable invariant sets.

I. INTRODUCTION

Following the line of research started in Ref. 29, in this paper we are going to complement the analysis performed in Refs. 14 and 41, where the presence of complex phenomena and strange attractors for two nonlinear Cournot triopoly game models with heterogeneous players has been shown via numerical simulations.

The method we will employ in our analysis of the models in Refs. 14 and 41 is the "Stretching Along the Paths" (from now on, SAP) technique, already used in Ref. 19 to rigorously prove the presence of chaos for some discrete-time one- and two-dimensional economic models of the classes of overlapping generations and duopoly games, as well as in Ref. 29 where the SAP method has been applied to the nonlinear Cournot triopoly game model with heterogeneous players introduced in Ref. 25. The SAP technique is called in this way because it concerns maps that expand the arcs along one direction and are instead compressive in the remaining directions. Differently from other methods for the search of fixed points and the detection of chaotic dynamics based on more sophisticated algebraic or geometric tools, such as the Conley index or the Lefschetz number (see, for instance, Refs. 13, 20, and 39), the SAP method relies on relatively elementary arguments and it is easy to apply in practical

[a)]Electronic mail: marina.pireddu@unimib.it. Tel.: +39 0264485767; FAX: +39 0264485705.

contexts, without the need of *ad-hoc* constructions. No differentiability conditions are required for the map describing the dynamical system under analysis and even continuity is needed only on particular subsets of its domain. Moreover, the function describing the considered dynamical system need not be one-to-one, like happens in the first model we analyze in Section III. We stress that in similar contexts it is in general not possible to apply the results for the Smale horseshoe, where one deals with homeomorphisms or diffeomorphisms. In fact, in the case of discrete-time dynamical systems we look for "topological horseshoes" (see, for instance, Refs. 7, 17, and 44]), i.e., a weaker version of the original Smale horseshoe in Ref. 38. The SAP technique can be used to rigorously prove the presence of chaos also for continuous-time dynamical systems, as done in Refs. 28 and 31, when the geometry of the system under analysis is related to that of the "Linked Twist Maps" (LTMs) (cf. Refs. 8, 12, and 32). See also Refs. 36 and 37 for recent three-dimensional continuous-time applications of the SAP method.

For the reader's convenience, we are going to recall in Section II what are the basic mathematical ingredients behind the SAP method, as well as the main conclusions it allows to draw about the chaotic features of the setting under analysis.

From a modeling viewpoint, both frameworks we analyze concern heterogeneous triopolies, where the three firms considered behave according to different strategies. In fact, in the absence of complete information, for instance on the shape of the demand function or on the competitors' future output choices, in such models it is assumed that at each time period firms decide how much to produce in the next period following different behavioral mechanisms. The models we deal with, taken from Refs. 14 and 41, are both extensions of the heterogeneous triopoly game framework studied in Ref. 15, in which the demand function and production costs are linear. More precisely, the model in Ref. 15 is modified in Ref. 14 assuming that production costs are quadratic, while in Ref. 41 the demand function becomes isoelastic.

We notice that the presence of an isoelastic demand function and linear production costs is shared also by the model introduced in Ref. 25 and further analyzed in Ref. 29, but the frameworks in Refs. 25 and 41 differ in the behavioral assumptions on one of the three firms, which in Ref. 25 is assumed to adopt a linear approximation mechanism, building a conjectured demand function on the basis of the local knowledge of the true demand function, while in Ref. 41 it is supposed to act adaptively, i.e., at each time it changes output proportionally to the difference between the naive expectation value and its previous output. In both works, one of the other two firms uses a gradient rule, i.e., it increases or decreases its output according to the sign of the marginal profit from the previous period, and the last firm adopts a best response mechanism under the assumption of naive expectations. As we shall see in Section III, the assumptions on the behavioral rules adopted in Ref. 14 coincide with those in Ref. 41 and are indeed the same as in Ref. 15.

The remainder of the paper is organized as follows. In Section II, we recall the main features of the SAP method. In Section III, after briefly presenting the triopoly game models taken from Refs. 14 and 41, we show how to apply the SAP technique to them. Some further considerations and comments about our method can be found in Section IV, which concludes the paper.

II. THE "STRETCHING ALONG THE PATHS" METHOD

In this section, we recall what the "Stretching along the paths" (SAP) technique consists in, referring the reader interested in further mathematical details to Ref. 30, where the original planar theory by Papini and Zanolin in Refs. 26 and 27 has been extended to the N-dimensional setting, with $N \geq 2$.

Since in Section III we will deal with three-dimensional settings only, we directly present the theoretical results we need in the special case in which $N = 3$. A more complete explanation of the three-dimensional context can be found in Ref. 29.

We start with some basic definitions.

A *path* in a metric space X is a continuous map $\gamma : [t_0, t_1] \to X$, for some $t_0 < t_1$. We also set $\bar{\gamma} := \gamma([t_0, t_1])$. Without loss of generality, we usually take the unit interval $[0, 1]$ as the domain of γ. A *sub-path* σ of γ is the restriction of γ to a compact sub-interval of its domain. By a *generalized parallelepiped* we mean a set $\mathcal{P} \subseteq X$ which is homeomorphic to the unit cube $I^3 := [0, 1]^3$ through a homeomorphism $h : \mathbb{R}^3 \supseteq I^3 \to \mathcal{P} \subseteq X$. We also set

$$\mathcal{P}_\ell^- := h([x_1 = 0]), \quad \mathcal{P}_r^- := h([x_1 = 1]),$$

and call them the *left* and the *right faces* of $\mathcal{P}$, respectively, where,[45] for $\alpha \in [0, 1]$,

$$[x_1 = \alpha] := \{(x_1, x_2, x_3) \in I^3 : x_1 = \alpha\}.$$

Setting

$$\mathcal{P}^- := \mathcal{P}_\ell^- \cup \mathcal{P}_r^-,$$

we call the pair

$$\tilde{\mathcal{P}} := (\mathcal{P}, \mathcal{P}^-)$$

an oriented parallelepiped of X.

Although in the applications discussed in the present paper the space X is simply $\mathbb{R}^3$ and the generalized parallelepipeds are standard parallelepipeds, the generality of our definitions makes them well suited for different contexts (see for instance Ref. 30, Figure 1).

We are now ready to introduce the *stretching along the paths* property for maps between oriented parallelepipeds.

Definition 2.1 (SAP). Let $\tilde{\mathcal{P}} := (\mathcal{P}, \mathcal{P}^-)$ and $\tilde{\mathcal{R}} := (\mathcal{R}, \mathcal{R}^-)$ be oriented parallelepipeds of a metric space X. Let also $\psi : \mathcal{P} \to X$ be a function and $\mathcal{K} \subseteq \mathcal{P}$ be a compact set. We say that $(\mathcal{K}, \psi)$ *stretches* $\tilde{\mathcal{P}}$ *to* $\tilde{\mathcal{R}}$ *along the paths*, and write

$$(\mathcal{K}, \psi) : \tilde{\mathcal{P}} \Subset \tilde{\mathcal{R}},$$

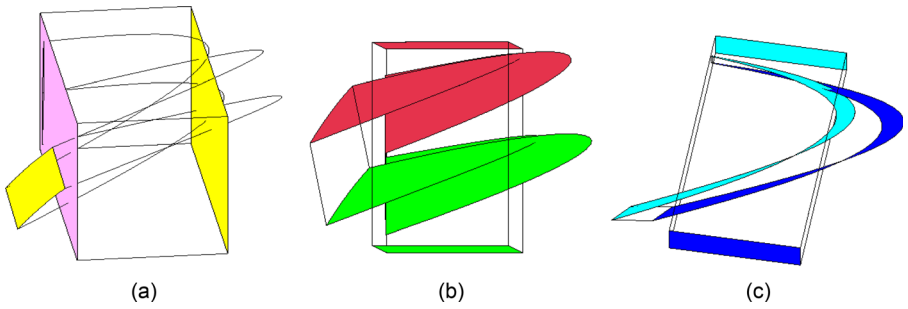

FIG. 1. An example of parallelepiped $\mathcal{R} \in \mathscr{R}$ satisfying conditions ($H1$)–($H5$) in Theorem 3.1. It has been oriented by taking as $\mathcal{R}^-$ the union of the two faces $\mathcal{R}_\ell^-$ (in lilac) and $\mathcal{R}_r^-$ (in yellow) in (a), defined in (3.7). Still in (a) we also represent $F(\mathcal{R}_\ell^-) \subset \mathcal{R}_\ell^-$ and $F(\mathcal{R}_r^-)$. In (b) and (c), we show how the other two pairs of opposite faces of $\mathcal{R}$ are transformed by the map F. We stress that in (c) we changed perspective, in order to better show the shape of the image sets. In (a)–(c), we used the same color to depict a set and its F-image set.

if the following conditions hold

- ψ is continuous on $\mathcal{K}$;
- for every path $\gamma : [0,1] \to \mathcal{P}$ with $\gamma(0)$ and $\gamma(1)$ belonging to different components of $\mathcal{P}^-$, there exists a sub-path $\sigma := \gamma|_{[t',t'']} : [0,1] \supseteq [t',t''] \to \mathcal{K}$, such that $\psi(\sigma(t)) \in \mathcal{R}$, $\forall\, t \in [t',t'']$, and, moreover, $\psi(\sigma(t'))$ and $\psi(\sigma(t''))$ belong to different components of $\mathcal{R}^-$.

See Ref. 29 for a description of the relationship between the SAP relation and other "covering relations" in the literature on topological dynamics. We just observe that the SAP relation is linked to the context of expansive-contractive maps, and, in particular, to the occurrence of topological horseshoes,[7,17,44] as it produces an expansion along one direction and a contraction along the remaining ones, differently from other extensions of the method of the turbulent maps in Ref. 5, which require an expansion along all the directions.[6,35]

A first crucial feature of the SAP relation is that, when Definition 2.1 is satisfied with $\tilde{\mathcal{P}} = \tilde{\mathcal{R}}$, it ensures the existence of a fixed point localized in the compact set $\mathcal{K}$ (cf. Ref. 30, Theorem 5.5 and see Ref. 30, Figure 1 for a graphical illustration). On the other hand, the most interesting case in view of detecting chaotic dynamics is when there exist at least two pairwise disjoint compact sets playing the role of $\mathcal{K}$ in Definition 2.1, because we then obtain a multiplicity of fixed points localized in those compact sets. Another crucial property of the SAP relation is that it is preserved under composition of maps, and thus, when dealing with the iterates of the function under consideration, it allows to detect the presence of periodic points of any period (for the precise statements, see Lemma A.1 and Theorem A.1 in Ref. 19, which can be directly transposed to the three-dimensional setting, keeping the same proofs).

Exploiting the just described properties of the SAP relation, it is possible to prove Theorem 2.1, which summarizes the conclusions that can be drawn when the SAP relation is fulfilled with $\tilde{\mathcal{P}} = \tilde{\mathcal{R}}$ for two disjoint compact sets playing the role of $\mathcal{K}$. Indeed, this will be the case in our applications in Section III, where Theorem 2.1 will represent our theoretical tool.

Theorem 2.1. *Let $\tilde{\mathcal{P}} := (\mathcal{P}, \mathcal{P}^-)$ be an oriented parallelepiped of a metric space X and let $\psi : \mathcal{P} \to X$ be a function. If $\mathcal{K}_0$ and $\mathcal{K}_1$ are disjoint compact subsets of $\mathcal{P}$ such that*

$$(\mathcal{K}_i, \psi) : \tilde{\mathcal{P}} \circlearrowright \tilde{\mathcal{P}}, \text{ for } i = 0, 1, \tag{2.1}$$

then ψ induces chaotic dynamics on two symbols on $\mathcal{P}$ relatively to $\mathcal{K}_0$ and $\mathcal{K}_1$, i.e., setting $\mathcal{K} := \mathcal{K}_0 \cup \mathcal{K}_1$ and introducing the nonempty compact set

$$\mathcal{I}_\infty := \bigcap_{n=0}^{\infty} \psi^{-n}(\mathcal{K}),$$

there exists a nonempty compact set

$$\mathcal{I} \subseteq \mathcal{I}_\infty \subseteq \mathcal{K},$$

on which the following properties are fulfilled:

(i) $\psi(\mathcal{I}) = \mathcal{I}$;

(ii) *$\psi|_{\mathcal{I}}$ is semi-conjugate to the Bernoulli shift on two symbols, that is, there exists a continuous onto map $\pi : \mathcal{I} \to \Sigma_2^+$, where $\Sigma_2^+ := \{0,1\}^{\mathbb{N}}$ is endowed with the distance*

$$\hat{d}(\boldsymbol{s}', \boldsymbol{s}'') := \sum_{i \in \mathbb{N}} \frac{d(s_i', s_i'')}{2^{i+1}}, \quad \text{for}$$

$$\boldsymbol{s}' = (s_i')_{i \in \mathbb{N}}, \boldsymbol{s}'' = (s_i'')_{i \in \mathbb{N}} \in \Sigma_2^+,$$

($d(\cdot,\cdot)$ is the discrete distance on $\{0,1\}$, i.e., $d(s_i', s_i'') = 0$ for $s_i' = s_i''$ and $d(s_i', s_i'') = 1$ for $s_i' \neq s_i''$), such that the diagram

$$\begin{array}{ccc} \mathcal{I} & \xrightarrow{\psi} & \mathcal{I} \\ \pi \downarrow & & \downarrow \pi \\ \Sigma_2^+ & \xrightarrow[\sigma]{} & \Sigma_2^+ \end{array}$$

commutes, where $\sigma : \Sigma_2^+ \to \Sigma_2^+$ is the Bernoulli shift defined by $\sigma((s_i)_i) := (s_{i+1})_i$, $\forall i \in \mathbb{N}$;

(iii) *the set of the periodic points of $\psi|_{\mathcal{I}_\infty}$ is dense in $\mathcal{I}$ and the inverse image set $\pi^{-1}(\boldsymbol{s}) \subseteq \mathcal{I}$ of every k-periodic sequence $\boldsymbol{s} = (s_i)_{i \in \mathbb{N}} \in \Sigma_2^+$ contains at least one k-periodic point.*

Remark 2.1. *According to Ref. 19, Theorem 2.2, from (ii) in Theorem 2.1 it follows that:*

- *$h_{\text{top}}(\psi) \geq h_{\text{top}}(\psi|_{\mathcal{I}}) \geq h_{\text{top}}(\sigma) = \log(2)$, where h_{top} is the topological entropy;*

- *there exists a nonempty compact invariant set* $\Lambda \subseteq \mathcal{I}$ *such that* $\psi|_\Lambda$ *is semi-conjugate to the Bernoulli shift on two symbols, topologically transitive and displays sensitive dependence on initial conditions.*

Moreover, if ψ *is also one-to-one on* $\mathcal{K}$*, then* ψ *restricted to a suitable invariant subset of* $\mathcal{K}$ *is semi-conjugate to the two-sided Bernoulli shift on two symbols* $\sigma : \Sigma_2 \to \Sigma_2$, $\sigma((s_i)_i) := (s_{i+1})_i$, $\forall i \in \mathbb{Z}$, *where* $\Sigma_2 := \{0,1\}^{\mathbb{Z}}$ *(see Ref. 31, Lemma 3.2).*[46]

We stress that an analogous counterpart of Theorem 2.1 holds when there are three or more pairwise disjoint compact sets[47] playing the role of $\mathcal{K}$ in Definition 2.1 and that both results can be proven using the same arguments employed for Ref. 19, Theorem 2.3.

We are now in position to explain what the SAP method consists in. Given a three-dimensional dynamical system generated by a map ψ, our technique consists in finding a subset $\mathcal{P}$ of the domain of ψ homeomorphic to the unit cube and (at least) two disjoint compact subsets of $\mathcal{P}$ with respect to which the stretching property in (2.1) is satisfied, once that $\mathcal{P}$ has been suitably oriented. In this way, Theorem 2.1 ensures the existence of chaotic dynamics for the system under consideration. In particular, Theorem 2.1 guarantees the positivity of the topological entropy for ψ, property which is generally considered as one of the trademark features of chaos.

This is the strategy we are going to adopt to analyze the models in Section III.

III. THE TRIOPOLY GAME MODELS

We apply the SAP method to two different economic models belonging to the class of triopoly games, taken, respectively, from Refs. 41 and 14.[48] With the term oligopoly economists denote a market form characterized by the presence of a small number of firms. Triopoly is a special kind of oligopoly where the firms involved are three. The term game refers to the fact that the firms make their decisions reacting to each other actual or expected moves, following a suitable strategy. In particular, we will deal with dynamic games where moves are repeated in time, at discrete, uniform intervals.

A. The model with isoelastic demand function

In the first model that we analyze, the economy consists of three firms producing an identical commodity at a constant unit cost, not necessarily equal for the three firms. The commodity is sold in a single market at a price which depends on total output through a given inverse demand function, which, like in Ref. 41, is supposed to be isoelastic.

The demand function is known globally to Firms 2 and 3, while Firm 1 does not know anything about the demand function and rather adopts a myopic adjustment mechanism, i.e., it increases or decreases its output according to the sign of the marginal profit from the last period.

The goal of each firm is the maximization of profits, i.e., the difference between revenue and costs. The problem of each firm is to decide at the beginning of every time period t how much to produce in the same period on the basis of the limited information available and, in particular, on the expectations about its competitors' future decisions.

In what follows, we introduce the needed notation[49] and the postulated assumptions:

(1) Notation

x_t: output of Firm 1 at time t;
y_t: output of Firm 2 at time t;
z_t: output of Firm 3 at time t;
p_t: unit price of the single commodity at time t.

(2) Inverse demand function

$$p_t := \frac{1}{x_t + y_t + z_t}. \tag{3.1}$$

(3) Technology

The unit cost of production for firm i is equal to c_i, $i = 1,2,3$, where c_1, c_2, c_3 are (possibly different) positive constants.

(4) Expectations

In the presence of incomplete information concerning their competitors' future decisions (and therefore about future prices), Firms 2 and 3 are assumed to use static expectations. This means that at each time t both Firms 2 and 3 expect that the other two firms will keep output unchanged with respect to the previous period.

Given such hypotheses concerning the expectations, Firm 2 is supposed to act as a best response player, choosing the output level that maximizes its expected profit. Firm 3 is instead an adaptive player, i.e., at each time it changes the output proportionally to the difference between the naive expectation value and its previous output.

As shown in Ref. 41, the assumptions above lead to the following system of three difference equations in the variables x, y, and z

$$\begin{cases} x_{t+1} = x_t + \alpha x_t \left(\dfrac{y_t + z_t}{(x_t + y_t + z_t)^2} - c_1 \right), \\ y_{t+1} = \sqrt{\dfrac{x_t + z_t}{c_2}} - (x_t + z_t), \\ z_{t+1} = (1-\lambda) z_t + \lambda \left(\sqrt{\dfrac{x_t + y_t}{c_3}} - (x_t + y_t) \right), \end{cases} \tag{3.2}$$

where α is a positive parameter denoting the speed of Firm 1's adjustment to changes in profit and $\lambda \in [0,1]$ describes how willing Firm 3 is to change its previous period production level.

We refer the interested reader to Ref. 41 for a more detailed explanation of the model, as well as for the derivation of (3.2).

In Ref. 41, Tramontana and Elsadany find two equilibrium solutions E_1 and E_2 for System (3.2), whose expression is given by

$$E_1 := \left(0, \frac{c_3}{(c_2+c_3)^2}, \frac{c_2}{(c_2+c_3)^2}\right), \tag{3.3}$$

and

$$E_2 := \left(\frac{2(c_2+c_3-c_1)}{(c_1+c_2+c_3)^2}, \frac{2(c_1+c_3-c_2)}{(c_1+c_2+c_3)^2}, \frac{2(c_1+c_2-c_3)}{(c_1+c_2+c_3)^2}\right), \tag{3.4}$$

study their local stability and provide numerical evidence of the presence of complex dynamics. In particular, they give conditions under which the Nash equilibrium point E_2 makes economic sense and show the existence of a double route to chaos for E_2, via flip bifurcations or via a Neimark-Sacker bifurcation.

They also find that parameter α plays a destabilizing role, but the kind of bifurcation undergone by E_2 when α increases depends on the relative values of the marginal costs. Indeed, if the firm adopting a myopic adjustment mechanism is the most efficient one, i.e., the value of c_1 is low with respect to the other marginal costs, then the Nash equilibrium loses stability via a Neimark-Sacker bifurcation, else, if the production efficiency differs less across the three firms, via a flip bifurcation. We stress that the former scenario is not present in the heterogeneous triopoly game studied in Ref. 14, we shall consider in Subsection III B, since, according to Ref. 41, it seems to be characteristic of the games with isoelastic demand function.

In order to apply the SAP method to show the existence of chaotic dynamics, and thus also of sensitive dependence on initial conditions, we will consider the setting illustrated in Ref. 41, Figure 3(b), where Tramontana and Elsadany find a Hénon-like attractor. In fact, in what follows we will integrate the study performed in Ref. 41 rigorously proving that, for suitable parameter configurations, System (3.2) exhibits chaotic behavior in the precise sense discussed in Section II.[50]

To such aim, setting $\mathbb{R}^{3*}_+ := \{(x,y,z) \in \mathbb{R}^3 : x \geq 0, y \geq 0, z \geq 0, (x,y,z) \neq (0,0,0)\}$, it is expedient to introduce the continuous map $F = (F_1, F_2, F_3) : \mathbb{R}^{3*}_+ \to \mathbb{R}^3$, with components

$$\begin{aligned} F_1(x,y,z) &:= x + \alpha x\left(\frac{y+z}{(x+y+z)^2} - c_1\right), \\ F_2(x,y,z) &:= \sqrt{\frac{x+z}{c_2}} - (x+z), \\ F_3(x,y,z) &:= (1-\lambda)z + \lambda\left(\sqrt{\frac{x+y}{c_3}} - (x+y)\right). \end{aligned} \tag{3.5}$$

We prove that the SAP property is satisfied for the map F when taking a generalized parallelepiped in the family $\mathscr{R}$ of (standard) parallelepipeds of the first orthant, whose elements are given by

$$\begin{aligned} \mathcal{R} = \mathcal{R}(x_i, y_i, z_i) = \{(x,y,z) \in \mathbb{R}^{3*}_+ : x_\ell \leq x \leq x_r, \\ y_\ell \leq y \leq y_r, z_\ell \leq z \leq z_r\}, \end{aligned} \tag{3.6}$$

with $x_\ell < x_r$, $y_\ell < y_r$, $z_\ell < z_r$ and x_i, y_i, z_i, $i \in \{\ell, r\}$, fulfilling the conditions in Theorem 3.1, and when orienting it by setting

$$\begin{aligned} \mathcal{R}^-_\ell &:= \{x_\ell\} \times [y_\ell, y_r] \times [z_\ell, z_r] \text{ and} \\ \mathcal{R}^-_r &:= \{x_r\} \times [y_\ell, y_r] \times [z_\ell, z_r]. \end{aligned} \tag{3.7}$$

Consistently with Ref. 41, we choose the marginal costs as $c_1 = 2.2$, $c_2 = 2.1$ and $c_3 = 1.63$, and $\lambda = 0.6$. On the other hand, in order to easily apply the SAP method, we need the parameter α to be close to 3.5, while in Ref. 41 the presence of a Hénon-like attractor is illustrated for α around 2.2. In fact, numerical exercises we performed show that when α increases it becomes easier to find a domain where to apply the SAP method. It would still be possible to apply our technique with a value for α lower than 3.5, at the cost of changing the parameter conditions in Theorem 3.1 and of making the computations in the proof much more complicated. However, it seems not possible to apply the SAP method to the first iterate of F when α is close to 2.2. The implications of this discrepancy will be discussed in Section IV.

Our result on System (3.2) reads as follows:

Theorem 3.1. *If the parameters of the map F defined in (3.5) assume the following values*

$$c_1 = 2.2,\ c_2 = 2.1,\ c_3 = 1.63,\ \lambda = 0.6,\ \alpha = 3.5, \tag{3.8}$$

then, for any parallelepiped $\mathcal{R} = \mathcal{R}(x_i, y_i, z_i)$ belonging to the family $\mathscr{R}$ described in (3.6), with x_i, y_i, z_i, $i \in \{\ell, r\}$, satisfying the conditions

$(H1)$ $x_\ell = 0$;

$(H2)$ $y_\ell + z_\ell \geq x_r \geq \sqrt{\dfrac{\alpha(y_\ell + z_\ell)}{\alpha c_1 - 1}} - (y_\ell + z_\ell) > 0$;

$(H3)$ $3\left(\sqrt{\dfrac{\alpha(y_r + z_r)}{\alpha c_1 + 2}} - (y_r + z_r)\right) > x_r$;

$(H4)$ $x_\ell + z_\ell \geq \dfrac{1}{4c_2}$, $y_r \geq \sqrt{\dfrac{x_\ell + z_\ell}{c_2}} - (x_\ell + z_\ell)$
$> \sqrt{\dfrac{x_r + z_r}{c_2}} - (x_r + z_r) \geq y_\ell > 0$;

$(H5)$ $x_r + y_r \geq \dfrac{1}{4c_3} \geq y_\ell$, $z_r \geq \dfrac{1}{4c_3}$,
$\sqrt{\dfrac{x_r + y_r}{c_3}} - (x_r + y_r)$
$\geq \sqrt{\dfrac{x_\ell + y_\ell}{c_3}} - (x_\ell + y_\ell) \geq z_\ell > 0$,

and oriented as in (3.7), there exist two disjoint compact subsets $\mathcal{K}_0 = \mathcal{K}_0(\mathcal{R})$ and $\mathcal{K}_1 = \mathcal{K}_1(\mathcal{R})$ of $\mathcal{R}$ such that

$$(\mathcal{K}_i, F) : \tilde{\mathcal{R}} \looparrowright \tilde{\mathcal{R}}, \text{ for } i = 0, 1. \tag{3.9}$$

Hence, the map F induces chaotic dynamics on two symbols on $\mathcal{R}$ relatively to $\mathcal{K}_0$ and $\mathcal{K}_1$ and displays all the properties listed in Theorem 2.1.

See Figure 1 for a possible choice of the oriented parallelepiped $\tilde{\mathcal{R}}$, together with its F-image set.

In Figure 2, we show how a path joining the left and right faces of $\mathcal{R}$ is transformed by the map F in (3.5), putting also in evidence the compact sets $\mathcal{K}_0$ and $\mathcal{K}_1$. In particular, in regard to Figure 2(b) we stress that, evaluating the

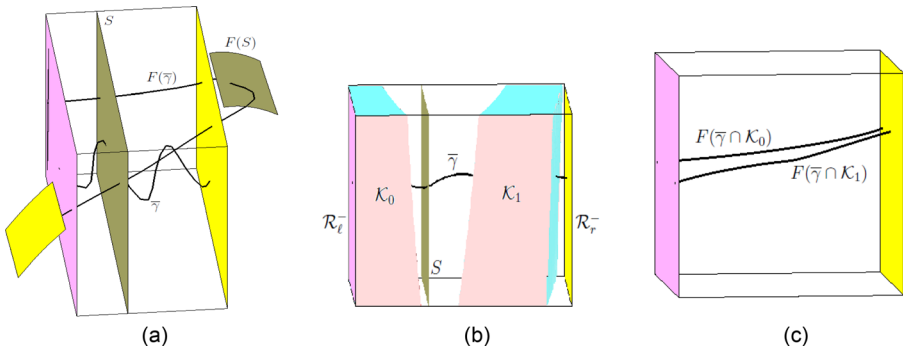

FIG. 2. With reference to the oriented parallelepiped $\tilde{\mathcal{R}}$ in Figure 1, we show in (a) that the F-image set of an arbitrary path γ joining in $\mathcal{R}$ the two components of the boundary set $\mathcal{R}^-$ intersects $\mathcal{R}$ twice. In particular, this is due to the fact that the vertical faces $\mathcal{R}_\ell^-$ and $\mathcal{R}_r^-$ are mapped by F on the left of or are contained in $\mathcal{R}_\ell^-$, in conformity with conditions $(C1)$ and $(C2)$ in the proof of Theorem 3.1, and that the vertical flat surface S is mapped by F on the right of $\mathcal{R}_r^-$, in agreement with condition $(C3')$ therein. Calling $\mathcal{R}_0$ and $\mathcal{R}_1$ the two parallelepipeds in which $\mathcal{R}$ is cut by S, we have that $\mathcal{K}_i := \mathcal{R}_i \cap F^{-1}(\mathcal{R})$, $i = 0, 1$, are the two disjoint compact sets in (b). As shown in the proof of Theorem 3.1, with such a choice it holds that $(\mathcal{K}_i, F) : \tilde{\mathcal{R}} \nleftrightarrow \tilde{\mathcal{R}}$, for $i = 0, 1$. Namely, for the arbitrary path γ in (a) joining in $\mathcal{R}$ its left and right faces, we show in (c) that the F-image sets of $\bar{\gamma} \cap \mathcal{K}_0$ and of $\bar{\gamma} \cap \mathcal{K}_1$ join $\mathcal{R}_\ell^-$ with $\mathcal{R}_r^-$, as required by the SAP property.

equilibrium points E_1 and E_2 in (3.3) and (3.4), respectively, at the parameter values considered in Theorem 3.1, it holds that $E_1 = (0, 0.117, 0.150) \in \mathcal{K}_0$ and $E_2 = (0.087, 0.098, 0.151) \in \mathcal{K}_1$. This is in agreement with the theoretical results recalled in Section II. Indeed, since in Theorem 3.1 we prove that the SAP property is satisfied with respect to two disjoint compact sets, then there exists (at least) a fixed point for the map F in each of them: on the other hand, since the map F has just two fixed points in $\mathbb{R}^{3*}_+$, i.e., E_1 and E_2, one of them has to lie in $\mathcal{K}_0$ and the other one in $\mathcal{K}_1$, as found.

Before proving Theorem 3.1, we make some comments on the conditions in $(H1)$–$(H5)$. First of all, we stress that those conditions imply that $x_\ell + y_\ell + z_\ell > 0$ and thus there are no issues with the definition of F on $\mathcal{R}$.[51] We also remark that we chose to split $(H1)$–$(H5)$ according to the corresponding conditions $(C1)$–$(C5)$ they allow to verify in the next proof. Moreover, we stress that the assumptions in $(H1)$–$(H5)$ are consistent, i.e., there exist parameter configurations satisfying them all. For instance, we checked that they are fulfilled for $c_1 = 2.2$, $c_2 = 2.1$, $c_3 = 1.63$, $\lambda = 0.6$, $\alpha = 3.5$, $x_\ell = 0$, $x_r = 0.118$, $y_\ell = 0.086$, $y_r = 0.120$, $z_\ell = 0.142$, $z_r = 0.154$. Indeed, these are the parameter values used to draw Figures 1 and 2. In particular, since $x_\ell = 0$, then $F(\mathcal{R}_\ell^-) \subset \mathcal{R}_\ell^-$ and thus only the black boundary of the set $F(\mathcal{R}_\ell^-)$ is visible in Figures 1(a) and 2(a).

Proof of Theorem 3.1. We show that, for the parameter values in (3.8), any choice of x_i, y_i, z_i, $i \in \{\ell, r\}$, fulfilling $(H1)$–$(H5)$ guarantees that the image under the map F of any path $\gamma = (\gamma_1, \gamma_2, \gamma_3) : [0, 1] \to \mathcal{R} = \mathcal{R}(x_i, y_i, z_i)$ joining the sets $\mathcal{R}_\ell^-$ and $\mathcal{R}_r^-$ defined in (3.7) satisfies the following conditions:

$$
\begin{aligned}
&(C1)\, F_1(\gamma(0)) \le x_\ell;\\
&(C2)\, F_1(\gamma(1)) \le x_\ell;\\
&(C3)\, \exists\, t^* \in (0,1) : F_1(\gamma(t^*)) > x_r;\\
&(C4)\, F_2(\gamma(t)) \subseteq [y_\ell, y_r],\ \forall t \in [0,1];\\
&(C5)\, F_3(\gamma(t)) \subseteq [z_\ell, z_r],\ \forall t \in [0,1].
\end{aligned}
$$

Broadly speaking, conditions $(C1)$–$(C3)$ describe an expansion with folding along the x–coordinate. In fact, the image $F \circ \gamma$ of any path γ joining in $\mathcal{R}$ the sides $\mathcal{R}_\ell^-$ and $\mathcal{R}_r^-$ horizontally crosses a first time the parallelepiped $\mathcal{R}$ for $t \in (0, t^*)$ and then crosses $\mathcal{R}$ back again for $t \in (t^*, 1)$. Conditions $(C4)$ and $(C5)$ imply instead a contraction along the y–coordinate and the z–coordinate, respectively.

Actually, in order to simplify our computations, instead of the necessary condition $(C3)$, we will check that the stronger requirement

$$
(C3')F_1\left(\frac{x_\ell + x_r}{3}, y, z\right) > x_r,\ \forall (y,z) \in [y_\ell, y_r] \times [z_\ell, z_r],
$$

is satisfied, which means that the inequality in $(C3)$ holds for any $t^* \in (0, 1)$ such that $\gamma(t^*) = ((x_\ell + x_r)/3, y, z)$, for some $(y, z) \in [y_\ell, y_r] \times [z_\ell, z_r]$. With this respect, notice that

$$
S := \left\{ \left(\frac{x_\ell + x_r}{3}, y, z \right) : (y,z) \in [y_\ell, y_r] \times [z_\ell, z_r] \right\} \subseteq \mathcal{R} \tag{3.10}
$$

is the green vertical surface depicted in Figures 2(a) and 2(b).

We claim that $(C1)$, $(C2)$, $(C3')$, $(C4)$ and $(C5)$ together imply (3.9) for

$$
\mathcal{K}_0 := \mathcal{R}_0 \cap F^{-1}(\mathcal{R}) \quad \text{and} \quad \mathcal{K}_1 := \mathcal{R}_1 \cap F^{-1}(\mathcal{R}), \tag{3.11}
$$

where

$$
\begin{aligned}
\mathcal{R}_0 := \Bigg\{ &(x,y,z) \in \mathbb{R}^3 : x \in \left[x_\ell, \frac{x_\ell + x_r}{3} \right],\\
&(y,z) \in [y_\ell, y_r] \times [z_\ell, z_r] \Bigg\},\\
\mathcal{R}_1 := \Bigg\{ &(x,y,z) \in \mathbb{R}^3 : x \in \left[\frac{x_\ell + x_r}{3}, x_r \right],\\
&(y,z) \in [y_\ell, y_r] \times [z_\ell, z_r] \Bigg\}
\end{aligned}
$$

(see Figure 2(b)). Notice at first that F is continuous on $\mathcal{K}_0 \cup \mathcal{K}_1$ because it is continuous on $\mathcal{R}$, and that $\mathcal{K}_0$ and $\mathcal{K}_1$ are compact because they are closed subsets of the compact sets

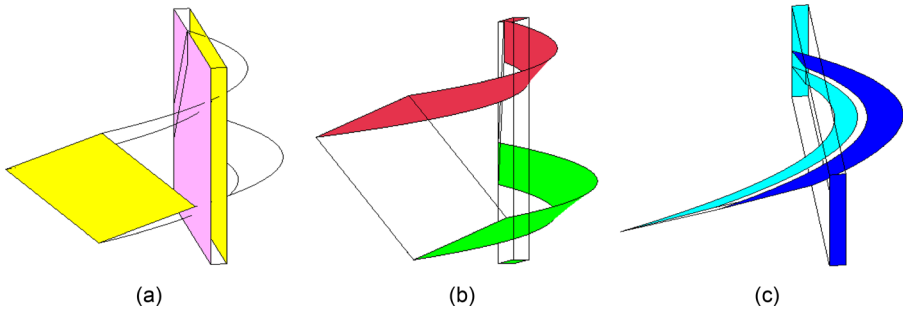

FIG. 3. An example of parallelepiped $\mathcal{R} \in \mathscr{R}$, satisfying conditions $(\mathcal{H}1)$–$(\mathcal{H}5)$ in Theorem 3.2. It has been oriented by taking as $\mathcal{R}^-$ the union of the two faces $\mathcal{R}_\ell^-$ (in lilac) and $\mathcal{R}_r^-$ (in yellow) in (a), defined in (3.7). Still in (a) we also represent $G(\mathcal{R}_\ell^-) \subset \mathcal{R}_\ell^-$ and $G(\mathcal{R}_r^-)$. In (b) and (c), we show how the other two pairs of opposite faces of $\mathcal{R}$ are transformed by the map G. We stress that in (c) we slightly changed perspective, in order to better show the shape of the image sets. In (a)–(c), we used the same color to depict a set and its G-image set.

$\mathcal{R}_0$ and $\mathcal{R}_1$, respectively. In order to show that $\mathcal{K}_0$ and $\mathcal{K}_1$ are disjoint, let us suppose by contradiction that there exists a point $P \in \mathcal{K}_0 \cap \mathcal{K}_1$. Then $P \in S$ and, since by condition $(C3')$ the set S in (3.10) is mapped by F outside $\mathcal{R}$ (see Figure 2(a)), then $F(P) \notin \mathcal{R}$, against (3.11). Furthermore, by $(C1)$, $(C2)$ and $(C3')$, for every path $\gamma : [0,1] \to \mathcal{R}$ such that $\gamma(0)$ and $\gamma(1)$ belong to different components of $\mathcal{R}^-$, there exist two disjoint sub-intervals $[t_0', t_0''], [t_1', t_1''] \subseteq [0,1]$ such that $\sigma_0 := \gamma|_{[t_0', t_0'']} : [t_0', t_0''] \to \mathcal{K}_0$, $\sigma_1 := \gamma|_{[t_1', t_1'']} : [t_1', t_1''] \to \mathcal{K}_1$, $F(\sigma_0(t_0'))$ and $F(\sigma_0(t_0''))$ belong to different components of $\mathcal{R}^-$, as well as $F(\sigma_1(t_1'))$ and $F(\sigma_1(t_1''))$. Moreover, from $(C4)$ and $(C5)$, it follows that $F(\sigma_0(t)) \in \mathcal{R}$, $\forall\, t \in [t_0', t_0'']$ and $F(\sigma_1(t)) \in \mathcal{R}$, $\forall\, t \in [t_1', t_1'']$.

This means that $(\mathcal{K}_i, F) : \tilde{\mathcal{R}} \nrightarrow \tilde{\mathcal{R}}$, $i = 0, 1$, and our claim is thus proved.

Once that the stretching condition in (3.9) is verified, the conclusion of the theorem follows by Theorem 2.1.[52]

In order to complete the proof, let us check that the choice of the parameters in (3.8) and of any domain $\mathcal{R} = \mathcal{R}(x_i, y_i, z_i)$ in agreement with $(H1)$–$(H5)$ implies that conditions $(C1), (C2), (C3'), (C4)$ and $(C5)$ are fulfilled for every path $\gamma : [0,1] \to \mathcal{R}$ joining $\mathcal{R}_\ell^-$ and $\mathcal{R}_r^-$. In so doing, we will prove that the inequality in $(C1)$ is indeed an equality. Just to fix the ideas, in what follows we will assume that $\gamma(0) \in \mathcal{R}_\ell^-$ and $\gamma(1) \in \mathcal{R}_r^-$.

Let us start with the verification of $(C1)$. By $(H1)$, $\gamma(0) \in \mathcal{R}_\ell^- = \{x_\ell\} \times [y_\ell, y_r] \times [z_\ell, z_r] = \{0\} \times [y_\ell, y_r] \times [z_\ell, z_r]$, and thus $\gamma_1(0) = 0$, so that, recalling the definition of F_1 in (3.5), it follows $0 = F_1(\gamma(0)) \le x_\ell = 0$, as desired.

In regard to $(C2)$, we have to verify that $F_1|_{\mathcal{R}_r^-} \le 0$, that is, $F_1(x_r, y, z) \le 0$, $\forall (y,z) \in [y_\ell, y_r] \times [z_\ell, z_r]$. Setting $A := y + z$, we consider, instead of $F_1|_{\mathcal{R}_r^-}$, the one-dimensional function

$$\phi : [y_\ell + z_\ell, y_r + z_r] \to \mathbb{R},$$
$$\phi(A) := x_r + \alpha x_r \left(\frac{A}{(x_r + A)^2} - c_1 \right).$$

Computing the first derivative of ϕ, we get $\phi'(A) = \alpha x_r((x_r - A)/(x_r + A)^3)$, which vanishes at $A = x_r$. However, since by $(H2)$ we have $y_\ell + z_\ell \ge x_r$, then $\phi'(A) \le 0$, $\forall A \in [y_\ell + z_\ell, y_r + z_r]$. Hence, $F_1|_{\mathcal{R}_r^-} \le F_1(x_r, y_\ell, z_\ell)$ and thus, in order to have $(C2)$ satisfied, it suffices that $F_1(x_r, y_\ell, z_\ell) \le 0$. Imposing such condition, we find $x_r + \alpha x_r(((y_\ell + z_\ell)/(x_r + y_\ell + z_\ell)^2) - c_1) \le 0$, which is fulfilled when $(\alpha c_1 - 1)/\alpha \ge (y_\ell + z_\ell)/(x_r + y_\ell + z_\ell)^2$. Making x_r explicit, this holds when $x_r \ge \sqrt{(\alpha(y_\ell + z_\ell))/(\alpha c_1 - 1)} - (y_\ell + z_\ell)$, that is, when $(H2)$ is fulfilled. Notice that the latter is a "true" restriction, since, still by $(H2)$, the right-hand side of the above inequality is positive. The verification of $(C2)$ is complete.

As regards $(C3')$, we need to check that $F_1((x_\ell + x_r)/3, y, z) > x_r$, $\forall (y,z) \in [y_\ell, y_r] \times [z_\ell, z_r]$, that is, recalling the definition of S in (3.10), $F_1|_S > x_r$. Notice that, by $(H1)$, $(x_\ell + x_r)/3 = x_r/3$. Analogously to what done above, instead of $F_1|_S$, let us consider the one-dimensional function

$$\varphi : [y_\ell + z_\ell, y_r + z_r] \to \mathbb{R},$$
$$\varphi(A) := \frac{x_r}{3} + \alpha \frac{x_r}{3} \left(\frac{A}{\left(\frac{x_r}{3} + A\right)^2} - c_1 \right).$$

Since by (H2) $y_\ell + z_\ell \ge x_r > x_r/3$, by the previous analysis we know that $\varphi(A) \ge \varphi(y_r + z_r) = F_1(x_r/3, y_r, z_r)$. Hence, in order to have $F_1|_S > x_r$, it suffices that $F_1(x_r/3, y_r, z_r) > x_r$, that is,

$$\frac{x_r}{3} \left(1 - \alpha c_1 + \frac{\alpha(y_r + z_r)}{\left(\frac{x_r}{3} + y_r + z_r\right)^2} \right) > x_r.$$

Since $x_r > 0$, making x_r explicit, we find

$$x_r < 3 \left(\sqrt{\frac{\alpha(y_r + z_r)}{\alpha c_1 + 2}} - (y_r + z_r) \right),$$

and this condition is satisfied thanks to $(H3)$. Hence $(C3')$ is verified.

In order to check $(C4)$, we need to show the two inequalities $F_2(x,y,z) \le y_r$, $\forall (x,y,z) \in \mathcal{R}$ and $F_2(x,y,z) \ge y_\ell$, $\forall (x,y,z) \in \mathcal{R}$, which are, respectively, satisfied if

$$\max_{(x,y,z) \in \mathcal{R}} F_2(x,y,z) \le y_r \quad \text{and} \quad \min_{(x,y,z) \in \mathcal{R}} F_2(x,y,z) \ge y_\ell. \tag{3.12}$$

Notice that such maximum and minimum values exist by Weierstrass Theorem.

Instead of $F_2|_{\mathcal{R}}$, setting $B := x + z$, we deal with the one-dimensional function

$$\psi : [x_\ell + z_\ell, x_r + z_r] \to \mathbb{R}, \quad \psi(B) := \sqrt{\frac{B}{c_2}} - B,$$

whose derivative is $\psi'(B) = (1/(2\sqrt{c_2 B})) - 1$. It vanishes at $\bar{B} = 1/(4c_2)$, which by $(H4)$ is not larger than $x_\ell + z_\ell$. Thus $\max_{(x,y,z)\in\mathcal{R}} F_2(x,y,z) = \psi(x_\ell + z_\ell)$ and $\min_{(x,y,z)\in\mathcal{R}} F_2(x,y,z) = \psi(x_r + z_r)$. Hence, the first condition in (3.12) is satisfied if $\psi(x_\ell + z_\ell) \le y_r$ and the second condition is fulfilled if $\psi(x_r + z_r) \ge y_\ell$. It is easy to see that both inequalities are fulfilled thanks to $(H4)$ and this concludes the verification of $(C4)$.

Let us finally turn to $(C5)$. In order to check it, we have to show that

$$\max_{(x,y,z)\in\mathcal{R}} F_3(x,y,z) \le z_r \text{ and } \min_{(x,y,z)\in\mathcal{R}} F_3(x,y,z) \ge z_\ell . \quad (3.13)$$

Instead of considering $F_3|_{\mathcal{R}}$, setting $D := x + y$ and $T := [x_\ell + y_\ell, x_r + y_r] \times [z_\ell, z_r]$, we deal with the two-dimensional function

$$\Phi : T \to \mathbb{R}, \quad \Phi(D,z) := (1-\lambda)z + \lambda\left(\sqrt{\frac{D}{c_3}} - D\right),$$

whose partial derivatives are

$$\frac{\partial\Phi}{\partial D} = \lambda\left(\frac{1}{2\sqrt{c_3 D}} - 1\right) \quad \text{and} \quad \frac{\partial\Phi}{\partial z} = 1 - \lambda .$$

If $\lambda \neq 1$ they do not vanish contemporaneously and thus there are no critical points in the interior of T. In this case, we study Φ on the boundary of its domain, obtaining the one-dimensional maps Φ_i, $i \in \{1,\dots,4\}$.

In regard to $\Phi_1(z) := \Phi|_{\{x_\ell+y_\ell\}\times[z_\ell,z_r]}(D,z) = \Phi(x_\ell + y_\ell, z)$, we have $\Phi_1'(z) = 1 - \lambda > 0$, and thus $\Phi_1(x)$ is increasing on $[z_\ell, z_r]$. Analogously, it holds that $\Phi_2(z) := \Phi|_{\{x_r+y_r\}\times[z_\ell,z_r]}(D,z) = \Phi(x_r + y_r, z)$ is increasing on $[z_\ell, z_r]$. As concerns $\Phi_3(D) := \Phi|_{[x_\ell+y_\ell,x_r+y_r]\times\{z_\ell\}}(D,z) = \Phi(D, z_\ell)$, we have that $\Phi_3'(D) = \lambda((1/(2\sqrt{c_3 D})) - 1)$, which vanishes at $\bar{D} = 1/(4c_3)$. This is the maximum point of Φ_3 if $\bar{D} \in [x_\ell + y_\ell, x_r + y_r]$. But that is guaranteed by the conditions in $(H5)$. Similarly, setting $\Phi_4(D) := \Phi|_{[x_\ell+y_\ell,x_r+y_r]\times\{z_r\}}(D,z) = \Phi(D, z_r)$, we find that its maximum point, still by $(H5)$, is given by $\bar{D}$.

Summarizing, the candidates for the maximum point of Φ on T are $(1/(4c_3), z_\ell)$ and $(1/(4c_3), z_r)$. Since $\Phi(1/(4c_3), z_\ell) < \Phi(1/(4c_3), z_r)$, $\max_{(x,y,z)\in\mathcal{R}} F_3(x,y,z) = \Phi(1/(4c_3), z_r)$. It is now easy to verify that the inequality $\Phi(1/(4c_3), z_r) \le z_r$ is satisfied when $z_r \ge 1/(4c_3)$, the latter being among the assumptions in $(H5)$.

The analysis above also suggests that the two candidates for the minimum point of Φ on T are $(x_\ell + y_\ell, z_\ell)$ and $(x_r + y_r, z_\ell)$. Since, again by $(H5)$, we have $\sqrt{(x_\ell + y_\ell)/c_3} - (x_\ell + y_\ell) \le \sqrt{(x_r + y_r)/c_3} - (x_r + y_r)$, then $\Phi(x_\ell + y_\ell, z_\ell) \le \Phi(x_r + y_r, z_\ell)$ and thus $\min_{(x,y,z)\in\mathcal{R}} F_3(x,y,z) = \Phi(x_\ell + y_\ell, z_\ell)$. The inequality $\min_{(x,y,z)\in\mathcal{R}} F_3(x,y,z) \ge z_\ell$ is then satisfied when $\sqrt{(x_\ell + y_\ell)/c_3} - (x_\ell + y_\ell) \ge z_\ell$, which is among the conditions in $(H5)$.

If $\lambda = 1$, the map F_3 does not depend on z and from the previous analysis we easily find that $\max_{(x,y,z)\in\mathcal{R}} F_3(x,y,z) = 1/(4c_3)$ and $\min_{(x,y,z)\in\mathcal{R}} F_3(x,y,z) = \sqrt{(x_\ell + y_\ell)/c_3} - (x_\ell + y_\ell)$. Imposing the conditions in (3.13), we obtain again the same requirements on the parameters found for the case $\lambda \neq 1$, and contained in $(H5)$. This concludes the verification of $(C5)$.

The proof is complete. □

Remark 3.1. *We stress that, slightly modifying the conditions for the construction of the parallelepiped $\mathcal{R}$ in the statement of Theorem 3.1, it is possible to obtain a robust result on the existence of chaotic dynamics, i.e., a result stable with respect to small changes in the value of the model parameters c_1, c_2, c_3, λ and α in (3.8). To such aim, it suffices to replace the weak inequalities in $(H2)$, $(H4)$ and (H5) with strict inequalities (and, correspondingly, set strict inequalities and inclusions in $(C2)$, $(C4)$ and (C5)) and exploit the continuity of the map F. Condition $(H3)$ and correspondingly $(C3)$ do not need any intervention, as they are already written in the "stricter" form. Notice that the parameter values in (3.8) together with the values for x_i, y_i, z_i, $i \in \{\ell, r\}$, used to draw Figures 1 and 2 satisfy even those stricter conditions. The only exception in that procedure is represented by (H1) (and, correspondingly, (C1)) that, in the specific example considered, cannot be rewritten using strict inequalities. This is due to the fact that, since the variable x represents an output, taking $x_\ell < 0$ would make no economic sense, while, as it is easy to verify, with $x_\ell > 0$ condition (C1) would not hold and the geometry required to apply the SAP method would be missing. On the other hand, $F_1(0,y,z) = 0$ for every $(y,z) \in \mathbb{R}^2_+$, and thus, under condition $(H1)$, $F_1(\mathcal{R}_\ell^-) = 0 = x_\ell$, independently of the choice of the model parameters. This means that, even if it is not possible to modify condition $(H1)$, the above suggested changes to $(H2)$, $(H4)$ and (H5) suffice to make Theorem 3.1 stable with respect to small perturbations in the parameter values.*

B. The model with quadratic production costs

In the second model that we analyze, taken from Ref. 14, the economy consists of three firms producing an identical commodity. Cost functions still can differ across firms and are quadratic in the quantities supplied. The commodity is sold in a single market at a price which depends on total output through a given inverse demand function, which is supposed to be linear.

Like for the model considered in Subsection III A, the demand function is known globally to Firms 2 and 3, while Firm 1 adopts a myopic adjustment mechanism.

The goal of each firm is the maximization of profits and, as in Ref. 41, the problem of each firm is to decide at the beginning of every time period t how much to produce in the same period on the basis of the limited information available.

The notation and the postulated assumptions are as follows:

(1) Notation

x_t: output of Firm 1 at time t;
y_t: output of Firm 2 at time t;
z_t: output of Firm 3 at time t;
p_t: unit price of the single commodity at time t.

(2) Inverse demand function

$$p_t := a - b(x_t + y_t + z_t)\,, \tag{3.14}$$

with a, b positive constants.

(3) Technology

Calling q_t the quantity supplied by a firm at time t, the production cost function for firm i at time t is equal to $C_{i,t} = c_i q_t^2$, $i = 1, 2, 3$, where c_1, c_2, c_3 are (possibly different) positive constants.

(4) Expectations

In the presence of incomplete information concerning their competitors' future decisions, Firms 2 and 3 are assumed to use naive expectations.

Given such hypotheses concerning the expectations, Firm 2 is supposed to act as a best response player, while Firm 3 is an adaptive player. Notice that, in the original version of the model in Ref. 14, Firm 2 is the adaptive player and Firm 3 the best response player. However, in view of simplifying the comparison with the framework in Subsection III A, we modified the ordering of the firms, as well as the notation with respect to Ref. 14, to make them consistent with those in the previous model.

As shown in Ref. 14, the assumptions above lead to the following system of three difference equations in the variables x, y and z:

$$\begin{cases} x_{t+1} = x_t + \alpha x_t\big(a - 2(b + c_1)x_t - b(y_t + z_t)\big), \\ y_{t+1} = \dfrac{1}{2(b + c_2)}(a - b(x_t + z_t)), \\ z_{t+1} = (1 - \lambda)z_t + \dfrac{\lambda}{2(b + c_3)}(a - b(x_t + y_t)), \end{cases} \tag{3.15}$$

where α is a positive parameter denoting the speed of Firm 1's adjustment to changes in profit and $\lambda \in [0, 1]$ describes how willing Firm 3 is to change its previous period production level. See Ref. 14 for a more detailed explanation of the model, as well as for the derivation of (3.15).

In Ref. 14 the authors find the two equilibrium solutions E_1^* and E_2^* for System (3.15), whose expression is given by

$$E_1^* := \left(0, \frac{a(b + 2c_3)}{3b^2 + 4b(c_2 + c_3) + 4c_2c_3}, \frac{a(b + 2c_2)}{3b^2 + 4b(c_2 + c_3) + 4c_2c_3}\right), \tag{3.16}$$

and

$$E_2^* := \left(\frac{a\big(b^2 + 2b(c_2 + c_3) + 4c_2c_3\big)}{2\big(2b^3 + 3b^2(c_1 + c_2 + c_3) + 4b(c_1c_2 + c_2c_3 + c_1c_3) + 4c_1c_2c_3\big)}, \frac{a\big(b^2 + 2b(c_1 + c_3) + 4c_1c_3\big)}{2\big(2b^3 + 3b^2(c_1 + c_2 + c_3) + 4b(c_1c_2 + c_2c_3 + c_1c_3) + 4c_1c_2c_3\big)}, \frac{a\big(b^2 + 2b(c_1 + c_2) + 4c_1c_2\big)}{2\big(2b^3 + 3b^2(c_1 + c_2 + c_3) + 4b(c_1c_2 + c_2c_3 + c_1c_3) + 4c_1c_2c_3\big)}\right), \tag{3.17}$$

study their local stability and provide numerical evidence of the presence of complex dynamics. In particular, they find that parameter α plays a destabilizing role and that the Nash equilibrium E_2^* loses stability only via a flip bifurcation. Moreover, in Ref. 14 the authors show how to apply the delay feedback control method by Pyragas[33] to control chaos and stabilize the dynamics.

In view of rigorously proving the existence of complex phenomena for System (3.15) in the sense discussed in Section II, we will consider the framework illustrated in Ref. 14, Figure 10, where Elabbasy *et al.* find a Hénon-like attractor.

Setting $\mathbb{R}^3_+ := \{(x, y, z) \in \mathbb{R}^3 : x \geq 0, y \geq 0, z \geq 0\}$, we introduce the continuous map $G = (G_1, G_2, G_3) : \mathbb{R}^3_+ \to \mathbb{R}^3$, with components

$$\begin{aligned} G_1(x, y, z) &:= x + \alpha x\big(a - 2(b + c_1)x - b(y + z)\big), \\ G_2(x, y, z) &:= \frac{1}{2(b + c_2)}(a - b(x + z)), \\ G_3(x, y, z) &:= (1 - \lambda)z + \frac{\lambda}{2(b + c_3)}(a - b(x + y)), \end{aligned} \tag{3.18}$$

and we show that the SAP property is satisfied for the map G when taking a generalized parallelepiped in the family $\mathscr{R}$ in (3.6), fulfilling the conditions in Theorem 3.2 and oriented as in (3.7).

In agreement with Ref. 14, we choose the marginal costs as $c_1 = 0.1$, $c_2 = 0.5$ and $c_3 = 0.3$, and $a = 10$, $b = 1$, $\lambda = 0.5$. On the other hand, in order to easily apply the SAP method we need the parameter α to be close to 3, while in Ref. 14 the presence of a Hénon-like attractor is numerically

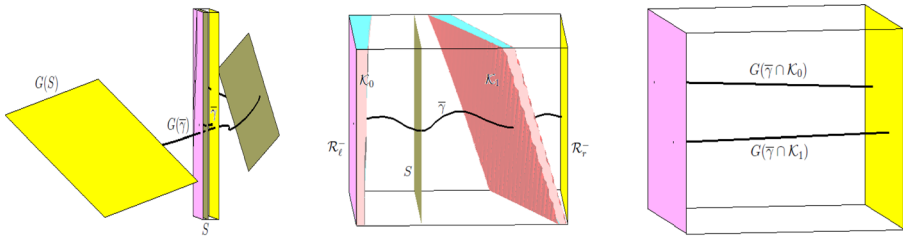

FIG. 4. With reference to the oriented parallelepiped $\tilde{\mathcal{R}}$ in Figure 3, we show in (a) that the G-image set of an arbitrary path γ joining in $\mathcal{R}$ the two components of the boundary set $\mathcal{R}^-$ intersects $\mathcal{R}$ twice. In particular, this is due to the fact that the faces $\mathcal{R}_\ell^-$ and $\mathcal{R}_r^-$ are mapped by G on the left of or are contained in $\mathcal{R}_\ell^-$, in conformity with conditions $(\mathcal{C}1)$ and $(\mathcal{C}2)$ in the proof of Theorem 3.2, and that the vertical flat surface S is mapped by G on the right of $\mathcal{R}_r^-$, in agreement with condition $(\mathcal{C}3')$ therein. Calling $\mathcal{R}_0$ and $\mathcal{R}_1$ the two parallelepipeds in which $\mathcal{R}$ is cut by S, we have that $\mathcal{K}_i := \mathcal{R}_i \cap G^{-1}(\mathcal{R})$, $i = 0, 1$, are the two disjoint compact sets in (b). With such a choice it holds that $(\mathcal{K}_i, G) : \tilde{\mathcal{R}} \twoheadrightarrow \tilde{\mathcal{R}}$, for $i = 0, 1$. Namely, for the arbitrary path γ in (a) joining in $\mathcal{R}$ the two components of $\mathcal{R}^-$, we show in (c) that the G-image sets of $\bar{\gamma} \cap \mathcal{K}_0$ and of $\bar{\gamma} \cap \mathcal{K}_1$ join $\mathcal{R}_\ell^-$ with $\mathcal{R}_r^-$, as required by the SAP property.

shown for α around 0.4. In fact, like happens with the model taken from Ref. 41, when α increases it becomes easier to find a domain where to apply the SAP technique, but, although it would be possible to slightly decrease the value of the reaction speed parameter, it seems not possible to apply the SAP method to the first iterate of G when α is close to 0.4.

Our result on System (3.15) reads as follows:

Theorem 3.2. *If the parameters of the map G defined in (3.18) assume the following values*

$$a = 10,\ b = 1,\ c_1 = 0.1,\ c_2 = 0.5,\\ c_3 = 0.3,\ \lambda = 0.5,\ \alpha = 3, \tag{3.19}$$

then, for any parallelepiped $\mathcal{R} = \mathcal{R}(x_i, y_i, z_i)$ belonging to the family $\mathscr{R}$ described in (3.6), with x_i, y_i, z_i, $i \in \{\ell, r\}$, satisfying the conditions

$$(\mathcal{H}1)\quad x_\ell = 0\,;$$

$$(\mathcal{H}2)\quad 0 < \frac{1 + \alpha a - 2\alpha(b + c_1)x_r}{\alpha b} \le y_\ell + z_\ell\,;$$

$$(\mathcal{H}3)\quad y_r + z_r < \frac{3\alpha a - 2\alpha(b + c_1)x_r - 6}{3\alpha b}\,;$$

$$(\mathcal{H}4)\quad 0 < \frac{a - 2(b + c_2)y_r}{b} \le x_\ell + z_\ell < x_r + z_r \le \frac{a - 2(b + c_2)y_\ell}{b}\,;$$

$$(\mathcal{H}5)\quad 0 < \frac{a - 2(b + c_3)z_r}{b} \le x_\ell + y_\ell < x_r + y_r \le \frac{a - 2(b + c_3)z_\ell}{b}\,,$$

and oriented as in (3.7), there exist two disjoint compact subsets $\mathcal{K}_0 = \mathcal{K}_0(\mathcal{R})$ and $\mathcal{K}_1 = \mathcal{K}_1(\mathcal{R})$ of $\mathcal{R}$ such that

$$(\mathcal{K}_i, G) : \tilde{\mathcal{R}} \twoheadrightarrow \tilde{\mathcal{R}},\ \text{for}\ i = 0, 1. \tag{3.20}$$

Hence, the map G induces chaotic dynamics on two symbols on $\mathcal{R}$ relatively to $\mathcal{K}_0$ and $\mathcal{K}_1$ and displays all the properties listed in Theorem 2.1.

See Figure 3 for a possible choice of the oriented parallelepiped $\tilde{\mathcal{R}}$ for System (3.15), together with its G-image set. In Figure 4, we show how a path joining the left and right faces of $\mathcal{R}$ is transformed by the map G in (3.18), putting also in evidence the compact sets $\mathcal{K}_0$ and $\mathcal{K}_1$. In particular, in regard to Figure 4(b), we notice that for the parameter values in (3.19) the equilibrium points E_1^* and E_2^* in (3.16) and (3.17), respectively, satisfy the conditions $E_1^* = (0, 2.35, 2.94) \in \mathcal{K}_0$ and $E_2^* = (2.81, 1.69, 2.11) \in \mathcal{K}_1$, in agreement with the theoretical results in Section II.

Before sketching the proof of Theorem 3.2, we make some comments on the conditions in $(\mathcal{H}1)$–$(\mathcal{H}5)$. First of all, we stress that they are consistent, i.e., there exist parameter configurations satisfying them all. For instance, we checked that they are fulfilled for $a = 10, b = 1, c_1 = 0.1, c_2 = 0.5, c_3 = 0.3, \lambda = 0.5, \alpha = 3, x_\ell = 0, x_r = 3.71, y_\ell = 0.9, y_r = 2.91, z_\ell = 1.28$ and $z_r = 3.5$. Indeed, these are the parameter values used to draw Figures 3–5. In particular, since $x_\ell = 0$, then $G(\mathcal{R}_\ell^-) \subset \mathcal{R}_\ell^-$ and thus only the black boundary of the set $G(\mathcal{R}_\ell^-)$ is visible in Figures 3(a) and 4(a).

Proof of Theorem 3.2. It is easy to check that, for the parameter values in (3.19), any choice of x_i, y_i, z_i, $i \in \{\ell, r\}$, fulfilling $(\mathcal{H}1)$–$(\mathcal{H}5)$ guarantees that the image under the map G of any path $\gamma = (\gamma_1, \gamma_2, \gamma_3) : [0, 1] \to \mathcal{R} = \mathcal{R}(x_i, y_i, z_i)$ joining $\mathcal{R}_\ell^-$ and $\mathcal{R}_r^-$ defined in (3.7) satisfies the following conditions:

$$(\mathcal{C}1)\ G_1(\gamma(0)) \le x_\ell\,;$$

$$(\mathcal{C}2)\ G_1(\gamma(1)) \le x_\ell\,;$$

$$(\mathcal{C}3)\ \exists\ t^* \in (0, 1) : G_1(\gamma(t^*)) > x_r\,;$$

$$(\mathcal{C}4)\ G_2(\gamma(t)) \subseteq [y_\ell, y_r],\ \forall t \in [0, 1]\,;$$

$$(\mathcal{C}5)\ G_3(\gamma(t)) \subseteq [z_\ell, z_r],\ \forall t \in [0, 1]\,.$$

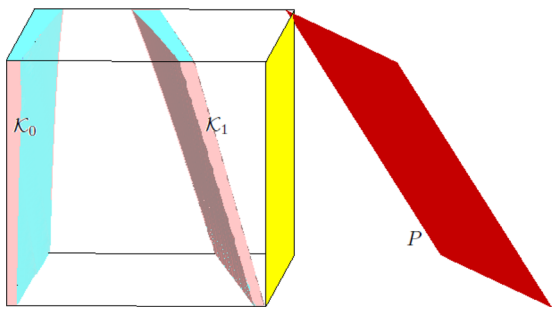

FIG. 5. The intersection between the plane P on which the price in (3.14) vanishes and the parallelepiped $\mathcal{R}$ represented in Figures 3 and 4 occurs outside $\mathcal{K} = \mathcal{K}_0 \cup \mathcal{K}_1$.

Actually, instead of the necessary condition $(\mathcal{C}3)$, assumption $(\mathcal{H}3)$ allows us to show the stronger requirement

$$(\mathcal{C}3')G_1\left(\frac{x_\ell + x_r}{3}, y, z\right) > x_r,\ \forall (y,z) \in [y_\ell, y_r] \times [z_\ell, z_r].$$

With this respect, notice that the set S introduced in (3.10) is the green vertical surface depicted in Figures 4(a) and 4(b).

As explained in the proof of Theorem 3.1, from the conditions above it follows that (3.20) is fulfilled, where $\mathcal{K}_0$ and $\mathcal{K}_1$ can be defined as in (3.11), just replacing F with G.

The conclusion of the theorem can then be achieved by applying Theorem 2.1. □

We stress that, as observed in Remark 3.1 in relation to Theorem 3.1, also Theorem 3.2 can be rewritten as a robust result on the existence of chaotic dynamics, just replacing the weak inequalities in $(\mathcal{H}2)$, $(\mathcal{H}4)$ and $(\mathcal{H}5)$ with strong inequalities.

We further notice that, since with respect to the framework introduced in Ref. 14 we switched the second and the third players and accordingly the values of c_2 and c_3, in Figures 3 and 4 we obtain a geometric framework similar to that in Figures 1 and 2. When considering instead the original model in Ref. 14, then, like in our setting, the first component would be expansive, and the second and the third ones would be contractive, but the behavior of the system along the y- and z-directions would be exchanged with respect to Figures 3(b) and 3(c).

Moreover, we remark that, although bearing a strong resemblance, Figures 1(c) and 3(c) differ in a crucial aspect: indeed, recalling the definition of $\mathcal{K}_0$ and $\mathcal{K}_1$ in (3.11), while in the former case F is not one-to-one on $\mathcal{K}_0$ and thus neither on $\mathcal{K} = \mathcal{K}_0 \cup \mathcal{K}_1$, in the latter setting G is one-to-one on $\mathcal{K}$, so that its restriction to a suitable invariant subset of $\mathcal{K}$ is semi-conjugate to the two-sided Bernoulli shift on two symbols, rather than to the one-sided shift.

We finally stress that in our analysis we should check that the price, determined through the inverse demand functions in (3.1) and (3.14), is positive for every output choice of the three firms we consider. While with (3.1) there are no negativity issues, it is easy to see that the lowest value that p in (3.14) assumes on the parallelepiped $\mathcal{R}$ in Figures 3 and 4, i.e., $p = a - b(x_r + y_r + z_r)$, is slightly negative. However, this is not a serious issue because, according to Theorem 2.1, the invariant set on which the interesting dynamics occur is contained in $\mathcal{K}$ and, as shown in Figure 5, the intersection between $\mathcal{K}$ and the plane $z = (a/b) - (x + y)$ on which the price in (3.14) vanishes is empty.

IV. CONCLUSIONS

In this paper, we have recalled what the SAP method consists in and we have applied that topological technique to rigorously prove the existence of robust chaotic sets for the triopoly game models introduced in Refs. 14 and 41. By "chaotic sets" we mean invariant domains on which the map describing the system under consideration is semi-conjugate to the Bernoulli shift (implying the features described in Remark 2.1) and where periodic points are dense. By "robustness" we mean that our result is stable with respect to small parameter perturbations. On the other hand, we stress that we could not say anything about the attractivity of those chaotic sets. In fact, in general, the SAP method does not allow to draw any conclusion in such direction. For instance, when performing numerical simulations for the parameter values in (3.8) and (3.19), no attractors appear on the computer screen. The same issue emerged with the two-dimensional models considered in Ref. 19 and with the three-dimensional model in Ref. 29. Both in the duopoly game model studied in Ref. 19 and in the triopoly game models analyzed in Ref. 29 and in the present paper, we are able to prove the presence of chaos for the parameter values considered in the literature, except for a bit larger speed of adjustment α. It makes economic sense that complex dynamics arise when firms are more reactive, but unfortunately for such parameter values no chaotic attractors can be found via numerical tools.

As explained in Ref. 29 taking as demonstrative example the well-known logistic map, this is not a limit of the SAP method: such issue is instead related to the necessity of working with the first iterate of the map generating the dynamical system under analysis to be able to perform computations by hands, especially when we deal with two- or three-dimensional systems. The simple example in Ref. 29 suggests indeed that dealing with higher-order iterates may allow to reach an agreement between the conditions required to employ the SAP method and those needed to find chaotic attractors via numerical simulations.

A suitable direction of future study can then be represented by the investigation of economically interesting but simple enough models, so that it is possible to work with higher-order iterates, in the attempt of rigorously proving the presence of chaos via the SAP technique for parameter values for which also computer simulations indicate the same kind of behavior.

In view of obtaining that same joint result, it is also possible to deal with maps bounding the dynamics and thus preventing divergence issues, even when instability regimes are reached. An example of this kind of map is given by the sigmoid function considered in Refs. 9, and 21–24, which limits the dynamics due to the presence of an upper and a lower horizontal asymptotes. A first attempt in such perspective would be the analysis of a two-dimensional model, in which the evolution of one component is regulated by the sigmoid function, while the other one can possibly be unbounded.

A further possible direction of future study is the analysis of continuous-time economic models with our technique, maybe in the context of LTMs, for systems switching between two different regimes, such as gross complements and gross substitutes.

ACKNOWLEDGMENTS

The author thanks the anonymous Reviewers for the helpful and valuable comments.

[1]H. N. Agiza, "Explicit stability zones for Cournot games with 3 and 4 competitors," Chaos Solitons Fractals **9**, 1955–1966 (1998).
[2]H. N. Agiza, "On the analysis of stability, bifurcation, chaos and chaos control of Kopel map," Chaos Solitons Fractals **10**, 1909–1916 (1999).

[3]A. Agliari, L. Gardini, and T. Puu, "The dynamics of a triopoly Cournot game," Chaos Solitons Fractals **11**, 2531–2560 (2000).
[4]G. I. Bischi and F. Tramontana, "Three-dimensional discrete-time Lotka-Volterra models with an application to industrial clusters," Commun. Nonlinear Sci. Numer. Simul. **15**, 3000–3014 (2010).
[5]L. S. Block and W. A. Coppel, "Stratification of continuous maps of an interval," Trans. Am. Math. Soc. **297**, 587–604 (1986).
[6]A. Blokh and E. Teoh, "How little is little enough?," Discrete Contin. Dyn. Syst. **9**, 969–978 (2003).
[7]K. Burns and H. Weiss, "A geometric criterion for positive topological entropy," Commun. Math. Phys. **172**, 95–118 (1995).
[8]R. Burton and R. W. Easton, "Ergodicity of linked twist maps," in *Theory of Dynamical Systems. Proceedings of an International Conference Held at Northwestern University*, Evanston, IL, 1979, Lecture Notes in Mathematics Vol. 819 (Springer, Berlin, 1980), pp. 35–49.
[9]F. Cavalli, A. Naimzada, and M. Pireddu, "Heterogeneity and the (de)stabilizing role of rationality," Chaos Solitons Fractals **79**, 226–244 (2015).
[10]C. Chiarella and F. Szidarovszky, "The asymptotic behavior of dynamic rent-seeking games," Comput. Math. Appl. **43**, 169–178 (2002).
[11]C. Chiarella and F. Szidarovszky, "Cournot oligopolies with product differentiation under uncertainty," Comput. Math. Appl. **50**, 413–424 (2005).
[12]R. L. Devaney, "Subshifts of finite type in linked twist mappings," Proc. Am. Math. Soc. **71**, 334–338 (1978).
[13]R. W. Easton, "Isolating blocks and symbolic dynamics," J. Differ. Equations **17**, 96–118 (1975).
[14]E. M. Elabbasy, H. N. Agiza, and A. A. Elsadany, "Analysis of nonlinear triopoly game with heterogeneous players," Comput. Math. Appl. **57**, 488–499 (2009).
[15]E. M. Elabbasy, H. N. Agiza, A. A. Elsadany, and H. EL-Metwally, "The dynamics of triopoly game with heterogeneous players," Int. J. Nonlinear Sci. **3**, 83–90 (2007).
[16]W. Ji, "Chaos and control of game model based on heterogeneous expectations in electric power triopoly," Discrete Dyn. Nat. Soc. **2009**, 469564.
[17]J. Kennedy and J. A. Yorke, "Topological horseshoes," Trans. Am. Math. Soc. **353**, 2513–2530 (2001).
[18]J. Ma and J. Zhang, "Price game and chaos control among three oligarchs with different rationalities in property insurance market," Chaos **22**, 043120 (2012).
[19]A. Medio, M. Pireddu, and F. Zanolin, "Chaotic dynamics for maps in one and two dimensions: A geometrical method and applications to Economics," Int. J. Bifurcation Chaos Appl. Sci. Eng. **19**, 3283–3309 (2009).
[20]K. Mischaikow and M. Mrozek, "Isolating neighborhoods and chaos," Jpn. J. Ind. Appl. Math. **12**, 205–236 (1995).
[21]A. Naimzada and M. Pireddu, "Dynamics in a nonlinear Keynesian good market model," Chaos **24**, 013142 (2014).
[22]A. Naimzada and M. Pireddu, "Dynamic behavior of product and stock markets with a varying degree of interaction," Econ. Modell. **41**, 191–197 (2014).
[23]A. Naimzada and M. Pireddu, "Real and financial interacting markets: A behavioral macro-model," Chaos Solitons Fractals **77**, 111–131 (2015).
[24]A. Naimzada and M. Pireddu, "Introducing a price variation limiter mechanism into a behavioral financial market model," Chaos **25**, 083112 (2015).
[25]A. Naimzada and F. Tramontana, "Two different routes to complex dynamics in an heterogeneous triopoly game," J. Differ. Equations Appl. **21**, 553–563 (2015).
[26]D. Papini and F. Zanolin, "On the periodic boundary value problem and chaotic-like dynamics for nonlinear Hill's equations," Adv. Nonlinear Stud. **4**, 71–91 (2004).
[27]D. Papini and F. Zanolin, "Fixed points, periodic points, and coin-tossing sequences for mappings defined on two-dimensional cells," Fixed Point Theory Appl. **2004**, 113–134.
[28]A. Pascoletti, M. Pireddu, and F. Zanolin, "Multiple periodic solutions and complex dynamics for second order ODEs via linked twist maps," in *Proceedings of the 8'th Colloquium on the Qualitative Theory of Differential Equations* [Electron. J. Qual. Theory Differ. Equations **14**, 1–32 (2008)].
[29]M. Pireddu, "Chaotic dynamics in three dimensions: A topological proof for a triopoly game model," Nonlinear Anal.: Real World Appl. **25**, 79–95 (2015).
[30]M. Pireddu and F. Zanolin, "Cutting surfaces and applications to periodic points and chaotic-like dynamics," Topol. Methods Nonlinear Anal. **30**, 279–319 (2007).
[31]M. Pireddu and F. Zanolin, "Chaotic dynamics in the Volterra predator-prey model via linked twist maps," Opuscula Math. **28**, 567–592 (2008).
[32]F. Przytycki, "Periodic points of linked twist mappings," Stud. Math. **83**, 1–18 (1986).
[33]K. Pyragas, "Continuous control of chaos by self-controlling feedback," Phys. Lett. A **170**, 421–428 (1992).
[34]H. Richter and A. Stolk, "Control of the triple chaotic attractor in a Cournot triopoly model," Chaos Solitons Fractals **20**, 409–413 (2004).
[35]R. Rudnicki, "Ergodic measures on topological spaces," Univ. Iagellonicae Acta Mathematica **26**, 231–237 (1987).
[36]A. Ruiz-Herrera and F. Zanolin, "An example of chaotic dynamics in 3D systems via stretching along paths," Ann. Mat. Pura Appl. **193**, 163–185 (2014).
[37]A. Ruiz-Herrera and F. Zanolin, "Horseshoes in 3D equations with applications to Lotka-Volterra systems," Nonlinear Differential Equations and Appl. **22**, 877–897 (2015).
[38]S. Smale, Diffeomorphism with many periodic points, in *Differential and Combinatorial Topology: A Symposium in Honor of Marston Morse* (Princeton University Press, Princeton, New Jersey, 1965), pp. 63–80.
[39]R. Srzednicki and K. Wójcik, "A geometric method for detecting chaotic dynamics," J. Differ. Equations **135**, 66–82 (1997).
[40]F. Szidarovszky and J. Zhao, "Dynamic oligopolies with intertemporal demand interaction," Comput. Math. Appl. **52**, 1623–1626 (2006).
[41]F. Tramontana and A. A. Elsadany, "Heterogeneous triopoly game with isoelastic demand function," Nonlinear Dyn. **68**, 187–193 (2012).
[42]F. Tramontana, L. Gardini, R. Dieci, and F. Westerhoff, "Global bifurcations in a three-dimensional financial model of bull and bear interactions," in *Nonlinear Dynamics in Economics, Finance and the Social Sciences* (Springer, Berlin, 2010), pp. 333–352.
[43]S. Yousefi, Y. Maistrenko, and S. Popovych, "Complex dynamics in a simple model of interdependent open economies," Discrete Dyn. Nat. Soc. **5**, 161–177 (2000).
[44]P. Zgliczyński and M. Gidea, "Covering relations for multidimensional dynamical systems," J. Differ. Equations **202**, 32–58 (2004).
[45]The choice of privileging the first coordinate in the definition of left and right faces of $\mathcal{P}$ has been made in view of our applications in Section III. On the other hand, any choice would give the same results, as it is possible to compose the homeomorphism h with a suitable permutation on three elements, without modifying its image set. For instance, the application considered in Ref. 29 made convenient privileging the third coordinate.
[46]As we shall see in Section III, this is not the case in the application in Subsection III A (cf. Figure 1), while it is the case in the application considered in Subsection III B (cf. Figure 3).
[47]Notice that the number of compact sets with respect to which the SAP property is satisfied coincides with the number of symbols in the semi-conjugate Bernoulli shift, as well as with the number of crossings between $\mathcal{P}$ and its ψ-image set.
[48]We stress that we chose to analyze first the model in Ref. 41 and then the one in Ref. 14, rather than following a chronological order, because, as it looks evident comparing the figures in Subsection III A with those in Subsection III B, the framework taken from Ref. 41 allows a clearer illustration and consequently an easier explanation. Hence, we will perform a detailed analysis of the model in Subsection III A, just sketching the main steps in the investigation of the model in Subsection III B and underlying some crucial differences between the two settings.
[49]We stress that, in order to make notation consistent between the two models we consider in Subsections III A and III B and in order to keep it as simple as possible, we modified with respect to Refs. 14 and 41 the letters used for some variables and parameters.
[50]Notice that we only prove *existence* of an invariant, chaotic set, not its *attractiveness*.
[51]Notice that, thanks to (*H1*)–(*H5*), it is immediate to check that also the functions we will introduce in the proof of Theorem 3.1 are well defined, even when not explicitly observed.
[52]Notice that, by the definition of $\mathcal{K}_0$ and $\mathcal{K}_1$, the invariant chaotic set $\mathcal{I} \subseteq \mathcal{K}_0 \cup \mathcal{K}_1$ in Theorem 2.1 lies entirely in the first orthant and thus makes economic sense for the considered application.